

Article

CO Oxidation Efficiency and Hysteresis Behavior over Mesoporous Pd/SiO₂ Catalyst

Rola Mohammad Al Soubaihi ¹, Khaled Mohammad Saoud ² , Myo Tay Zar Myint ³, Mats A. Göthelid ⁴  and Joydeep Dutta ^{1,*} 

¹ Functional Materials, Applied Physics Department, School of Engineering Sciences, KTH Royal Institute of Technology, AlbaNova Universitetscentrum, 106 91 Stockholm, Sweden; rolaas@kth.se

² Liberal Arts and Sciences Program, Virginia Commonwealth University in Qatar, Doha, Qatar; s2kmsaou@vcu.edu

³ Department of Physics, College of Science, Sultan Qaboos University, P.O. Box 36, Muscat PC 123, Oman; myotayzar.myint@gmail.com

⁴ Materialfysik, SCI, Albano, Hannes Alfvéns väg 12, KTH Royal Institute of Technology, 114 19 Stockholm, Sweden; gothelid@kth.se

* Correspondence: joydeep@kth.se

Abstract: Carbon monoxide (CO) oxidation is considered an important reaction in heterogeneous industrial catalysis and has been extensively studied. Pd supported on SiO₂ aerogel catalysts exhibit good catalytic activity toward this reaction owing to their CO bond activation capability and thermal stability. Pd/SiO₂ catalysts were investigated using carbon monoxide (CO) oxidation as a model reaction. The catalyst becomes active, and the conversion increases after the temperature reaches the ignition temperature (T_{ig}). A normal hysteresis in carbon monoxide (CO) oxidation has been observed, where the catalysts continue to exhibit high catalytic activity (CO conversion remains at 100%) during the extinction even at temperatures lower than T_{ig}. The catalyst was characterized using BET, TEM, XPS, TGA-DSC, and FTIR. In this work, the influence of pretreatment conditions and stability of the active sites on the catalytic activity and hysteresis is presented. The CO oxidation on the Pd/SiO₂ catalyst has been attributed to the dissociative adsorption of molecular oxygen and the activation of the C-O bond, followed by diffusion of adsorbates at T_{ig} to form CO₂. Whereas, the hysteresis has been explained by the enhanced stability of the active site caused by thermal effects, pretreatment conditions, Pd-SiO₂ support interaction, and PdO formation and decomposition.

Keywords: CO oxidation; hysteresis; thermal stability; pretreatment; structure-activity



Citation: Al Soubaihi, R.M.; Saoud, K.M.; Myint, M.T.Z.; Göthelid, M.A.; Dutta, J. CO Oxidation Efficiency and Hysteresis Behavior over Mesoporous Pd/SiO₂ Catalyst. *Catalysts* **2021**, *11*, 131. <https://doi.org/10.3390/catal11010131>

Received: 16 December 2020

Accepted: 13 January 2021

Published: 16 January 2021

Publisher's Note: MDPI stays neutral with regard to jurisdictional claims in published maps and institutional affiliations.



Copyright: © 2021 by the authors. Licensee MDPI, Basel, Switzerland. This article is an open access article distributed under the terms and conditions of the Creative Commons Attribution (CC BY) license (<https://creativecommons.org/licenses/by/4.0/>).

1. Introduction

Low-temperature carbon monoxide (CO) oxidation is considered a prototype reaction for heterogeneous catalysis. It has garnered attention in recent years due to its interesting catalytic behavior and the screening of new heterogeneous catalysts [1]. In recent years, “metal oxide supported palladium catalysts” have been studied in detail due to their high intrinsic activity, lower cost, metal-support interaction, and other non-linear dynamic behaviors, which are beneficial for CO oxidation [2,3]. The properties of Pd catalysts are affected by types of support, preparation conditions, and the dispersion of the Pd particles [4]. Support materials are a crucial factor in the catalytic behavior of Pd toward CO oxidation where the synergistic effect between Pd and the support depends on the nature of support (i.e., reducible vs. non-reducible) [5]. Stabilization of the catalyst can be attained by anchoring Pd particles on the surface of the support to resist sintering at high temperatures and dispersion in metal oxides, such as silica (SiO₂) [6]. Silica materials have been widely explored as catalyst support owing to their unique morphologies, narrow pore sizes, large surface areas, and thermal stability [6]. Despite being inert and irreducible, SiO₂ can exhibit a metal-support interaction with Pd, that affects the morphology, wetting,

and interdiffusion in the Pd/SiO₂ catalyst, which is known to improve catalytic properties and stability [7]. The heat treatment under oxidation and reduction conditions is crucial for the preparation of supported Pd/SiO₂ catalysts. Such treatment can induce morphological changes and affect the dispersion of Pd particles resulting from the sintering of the Pd particles. Therefore, it is crucial to study the optimal preparation and pretreatment conditions and activation of the Pd catalysts. Morphological changes due to sintering have been reported wherein encapsulation, inter-diffusion, and alloy formation are found to be highly dependent on heating conditions [8]. The thermal treatment can cause deactivation of catalysts impacting the support, oxidation state, particle size, and the surface area of the catalyst due to sintering at high temperatures, which can directly influence the catalytic activity [2]. Palladium nanoparticles dispersion within a narrow pore size distribution and high surface area mesoporous silica (SiO₂) aerogel increases the catalytic activity of supported Pd catalysts. Moreover, the formation of Pd intermediate has been reported to influence the catalytic behavior and stability during ignition/extinction cycles [9]. The Pd catalyst has a wide operating temperature range during CO oxidation and can exist in two thermodynamically stable phases depending on the partial pressure of oxygen and the reaction temperature, either as palladium oxide (PdO) or in its metallic form (Pd) [10]. Therefore, the Pd catalyst exhibits nonlinear dynamics such as hysteresis effects and self-sustained oscillations due to the PdO decomposition and re-formation. This behavior could be crucial for the future development of heterogeneous catalysts for a range of reactions in addition to CO oxidation reactions [11].

Hysteresis is a complex phenomenon attributed to many factors such as surface coverage, multiplicity, thermal inertia, exotherm, and catalyst oxidation states. The effects of CO conversion hysteresis over supported and unsupported palladium catalysts were investigated and reported by researchers, including our group [2,12]. Hysteresis loops arise from the difference between the activity during the heating and cooling processes [13]. The reversible oxidation of Pd due to the dissociative adsorption of oxygen on the sub-surface layer of the catalyst to form a surface layer of PdO leads to the hysteresis and self-sustained oscillations in CO oxidation [12]. This phenomenon was observed in many exothermic oxidation reactions in addition to CO oxidation and has been attributed to the heat released at the surface of the catalyst during the exothermic oxidation, wherein the surface temperature exceeds the reactor temperature [14]. "Normal" hysteresis observed in CO oxidation when the catalytic activity during CO ignition takes place at a higher temperature than the temperature during extinction, while inverse hysteresis is observed for some gas mixtures, where the catalytic activity during ignition exceeds the activity during extinction [15]. This behavior has been realized and plays a crucial role in many applications, including long-life carbon dioxide (CO₂) lasers, partial oxidation in chemical synthesis, and removal of pollutants in catalytic converters during prototype exothermic reactions including CO oxidation [16]. Most of the reports in the literature focus on the CO hysteresis as a function of inlet temperatures [15]. Although reasons for the hysteresis phenomena are still unclear, some researchers associate its rise with the multiplicity of steady states, oxidation of the catalyst, and temperature fluctuations. Due to the coexistence of PdO or Pd states in the palladium catalyst and the strong interdependence of catalytic activity and hysteresis on the support materials, palladium catalysts exhibit normal hysteresis during CO oxidation due to the decomposition and reformation of PdO.

In our previous work, we have reported the synthesis and the catalytic activity of the Pd/SiO₂ catalyst. In continuation of this work, we provide detailed information on the influence of pretreatment conditions on the catalyst microstructure and dispersion of Pd, thermal stability, and catalyst performance. The mesoporous Pd/SiO₂ aerogel catalyst with well-dispersed Pd nanoparticles was evaluated for CO oxidation under ignition/extinction conditions, wherein the possibility of using the hysteresis effect to attain high conversions at lower reaction temperatures were explored. The Pd/SiO₂ catalyst is a CO oxidation catalyst with high catalytic activity at a temperature range of (150 to 250 °C). It has excellent thermal stability, which could stabilize the active phase for CO oxidation by

increasing the metal-support interaction and dispersion of Pd species. This study reports the experimental data on the catalytic activity, hysteresis, and thermal stability during the CO oxidation over the Pd/SiO₂ catalyst, which is found to be intensely dependent on the preparation, pretreatment conditions, and external parameters. The preparation and treatment conditions' effect under dynamic reaction conditions provide a correlation between the catalyst structure and activity, as well as the role of thermal effects on the observed hysteresis behavior.

2. Results and Discussion

2.1. Catalytic Activity and Hysteresis Behavior of Pd/SiO₂ Catalysts

2.1.1. CO Conversion Efficiency and Light-Off Testing

Catalytic CO oxidation was performed under constant gas composition where the concentration of CO is 3.5%, with a surplus of oxygen (20% concentration) balanced in helium to allow for the complete CO conversion. The result was obtained under controlled heating (heating rate is 10 °C/min), and subsequent normal cooling conditions (ignition/extinction) as a function of the reaction (catalyst) temperature and not the feed gas inlet temperature, as reported by other researchers in this field [17]. In this context, we defined the ignition or light-off temperature (T_{ig}) as the temperature at which the CO conversion efficiency reaches 3% during heating and extinction or light-out temperature (T_{ext}) as the temperature at which the CO conversion efficiency reaches 3% during cooling. Furthermore, we define the hysteresis as the difference between the temperatures at which the CO conversion efficiency is 50% during ignition and extinction.

Figure 1a presents the conversion efficiency and catalyst temperature during the catalytic CO conversion test as a function of time, while Figure 1b shows the conversion efficiency as a function of the catalyst temperature for two consecutive light-off cycles. The figures show clearly the exothermic evolution as a function of time and the hysteresis effect for oxidation reaction. During heating (ignition), three active conversion zones can be distinguished in which the reaction takes place at varying catalyst temperatures. In Zone I, when the catalyst temperature is below 214 °C, the reaction rate is slow, leading to low CO conversion as it is kinetically controlled. In Zone II, intermediate conversion zone when the temperature is above 214 °C, the reaction rate is slightly higher, leading to better CO conversions as it is controlled by internal diffusion and mass transfer limitations in the SiO₂ porous support [18]. In Zone III, the full conversion zone when the temperature increased to above 276 °C, at which the CO conversion efficiency reaches 50%, the reaction rate is high and controlled by external (gas phase) diffusion without any mass transfer limitations.

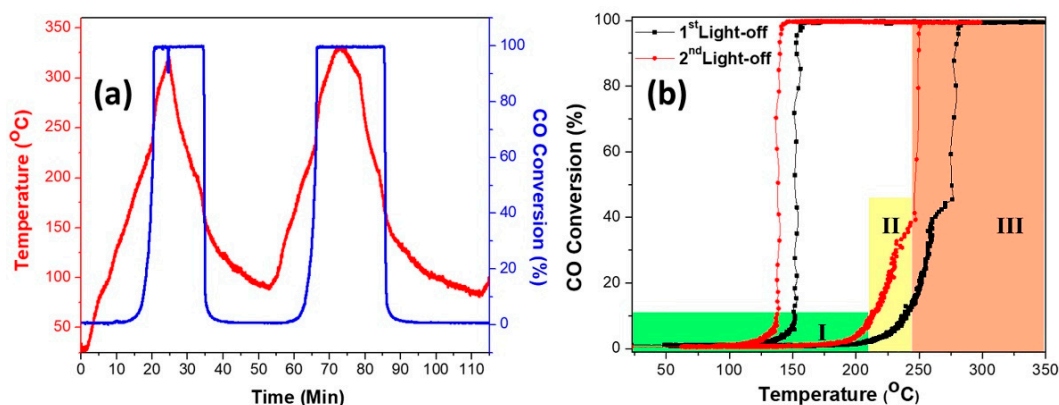


Figure 1. (a) Reaction temperature and carbon monoxide (CO) conversion efficiency during typical light-off testing in a synthetic gas reactor as a function of time, (b) CO conversion efficiency, and hysteresis effect as a function of the reaction (catalyst) temperature.

On the other hand, during cooling (extinction), the reaction kinetics and diffusion of gas molecules play a role due to temperature differences between the high exothermic reaction heat generated at the catalyst surface and the reduced gas temperature at the reactor inlet, when the reactor is below the ignition temperature (below 214 °C). This leads to kinetic bi-stability, where the surface nanoparticles alternate between active (PdO) and in-active (Pd) states [19]. The self-sustained oscillations and hysteresis appear during cooling of the catalyst under the flow of the reaction gas mixture. The cycling experiments for the first and second light-off were performed, where the first ignition was obtained at 88.6 °C. These results confirm that the hysteresis effect could help attain and maintain high CO conversions while oscillating between higher and lower temperatures. Upon heating/cooling, a significant hysteresis was observed at 121–296 °C. This effect can help in reducing the temperature for the second light-off for CO conversions over a Pd/SiO₂ catalyst by lowering the temperature along the extinction leg to a point below the ignition temperature as a result of the convective heat transfer associated with the temperature of the incoming gas, the CO oxidation reaction exotherm, and conduction of heat along the catalyst. Table 1 summarizes and compares the catalytic ignition and extinction profile and hysteresis width of the Pd/SiO₂ aerogel catalyst during the first light-off (fresh catalyst) and the second light-off (heat-treated catalyst in the CO/O₂ mixture) cycles. The second light-off demonstrated higher activity compared to the first light-off cycle, as shown in Figure 1b. The temperature of the second light-off and hysteresis width were shifted to lower values compared to the first light-off cycle. Reportedly, Pd⁰ metal particles are preferably formed under a reducing CO atmosphere, whereas, under oxidizing O₂ atmosphere, Pd²⁺ or PdO particles should be formed [20]. The heating in the CO/O₂ mixture caused the CO conversion ignition temperature (T_{ig}) of Pd/SiO₂ to decrease from 214 to 195 °C, and the full CO conversion was achieved at (T_{100}) of 272 °C rather than 296 °C, while the hysteresis width decreased from 121 to 108 °C. The results might be attributed to the removal of moisture and hydrocarbons from the surface of the catalyst, increasing the metal-support interaction, as observed in XPS and XRD [2], the formation of palladium silicide, reduction of metal hydroxide, and oxidation of metallic Pd lead to improving the active site for the CO oxidation reaction.

Table 1. Comparison between the catalytic ignition and extinction profile, and hysteresis width of Pd/SiO₂ aerogel catalysts of the first and the second light-off (ignition) cycles.

Light-Off Cycle	T_{ig} (°C)	T_{50} (°C)	T_{100} (°C)	T_{ex} (°C)	Hysteresis Width (°C)
First light-off	214	276	296	138	121
Second light-off	195	247	272	123	108

Where T_{ig} is the ignition temperature at 3% conversion in °C, T_{50} is the temperature at 50% conversion in °C, T_{100} is the temperature at 100% conversion in °C, T_{ex} is the extinction temperature at 3% conversion in °C, and hysteresis width is at 50% conversion in °C.

Furthermore, the removal of silanol groups increases the metal dispersion and the catalytic activity of the Pd/SiO₂ catalyst [21]. Note that the conversion curve remained the same even after four cycles. The effect of heating rate on the catalytic activity, hysteresis, and ignition/extinction profile of the Pd/SiO₂ aerogel catalyst will be reported in a future manuscript.

To further investigate the catalytic activity and hysteresis behavior of the catalyst during the first and second light-off (or before and after catalytic conversion experiments), changes in the catalyst's porosity, surface area, Pd particle size, the oxidation state of Pd, crystallography, and pore size were investigated before and after the CO oxidation reaction.

The porosity of the catalyst assumes a role in the catalytic activity and the hysteresis activity during the CO oxidation reaction. The N₂ adsorption-desorption characteristics of fresh (as prepared) Pd/SiO₂ aerogel isotherms and pore size distribution before the CO oxidation reaction was performed. The isotherms of the fresh sample with the N₂ uptake consistent with type IV (according to the IUPAC classification), and a narrow H₂ type hysteresis loop at $p/p_0 > 0.75$ are shown in Figure S1, suggesting mesoporous and microporous characteristics due to capillary condensation in silica [22]. The increment of adsorption at $p/p_0 = 1.0$ was caused by larger mesopores, typical in mesoporous materials [23]. This wider hysteresis loop is known to occur when the distributions of the pore radius are wide [24]. The effect of heat treatment in the CO/O₂ atmosphere (after the first light-off) on the morphologies, surface area, and pore volume distributions were investigated to clarify the higher catalytic activity in the second light-off observed for CO oxidation on the Pd/SiO₂ catalyst. The structural properties of both samples were shown in Table 2 and illustrated in Figure S1. The fresh Pd/SiO₂ aerogel catalyst shows continuous pore volume distribution with diameters between 2 and 80 nm. However, N₂ adsorption-desorption characteristics of the Pd/SiO₂ aerogel pore size distribution after CO oxidation (after the first light-off) show a pore volume with continuous distribution of pore diameters (between 2 and 60 nm). The higher temperature during the CO oxidation does not affect the integrity of the catalyst. However, the quantity of large mesopores and macropores is eliminated due to the collapse following the heat treatment, leading to a higher ratio of micropores and small mesopores, as reported by Gage et al. [25]. BET results show that the average pore diameter of the Pd/SiO₂ aerogel slightly reduced to 15.6 nm and the pore volume slightly increased to 0.06 cm³/g, although the surface area reduced to ~940.9 m²/g. The decrease in the surface area could be attributed to the sintering of the large excess palladium particles outside the pores as found in electron microscopy, which will be discussed later.

Table 2. Structural properties of fresh Pd/SiO₂ aerogel catalysts and after the first light-off.

Catalyst Pd/SiO ₂	BET Surface Area (gm ⁻¹)	Pore Diameter ^a (nm)	Pore Volume ^a (cm ³ g ⁻¹)
Fresh	1113.65	15.7	0.05
After the first light-off	940.86	15.6	0.06

^a Calculated by the Barrett, Joyner, and Halenda (BJH) method from the desorption isotherm.

To study the effect of the particles size of the catalyst on the catalytic activity and hysteresis width during the CO oxidation reaction, the TEM of the catalyst before (fresh) (Figure 2a) and after CO oxidation (first light-off) (Figure 2b) was performed. The presence of a large number of smaller Pd particles (2–5 nm) in the framework (marked by yellow arrows) located inside the mesoporous framework of SiO₂ aerogels homogeneously dispersed within the SiO₂ network and a few large surface particles (20–40 nm) (marked by magenta arrows). This unique texture is believed to occur due in the samples prepared by the sol-gel synthesis resulting in a better catalytic activity and effectively hindering the sintering of Pd particles [26]. The average size estimated from over 200 particles shows a mean size of the Pd particles in as-synthesized particles as 6.1 nm. Figure 2d,e shows the TEM micrographs of typical samples after CO oxidation. The mean size of Pd particles following the completion of the reaction was found to grow to ~7.8 nm due to the sintering, as also observed from the X-ray diffraction (XRD) analysis, and reported in a previous work [2].

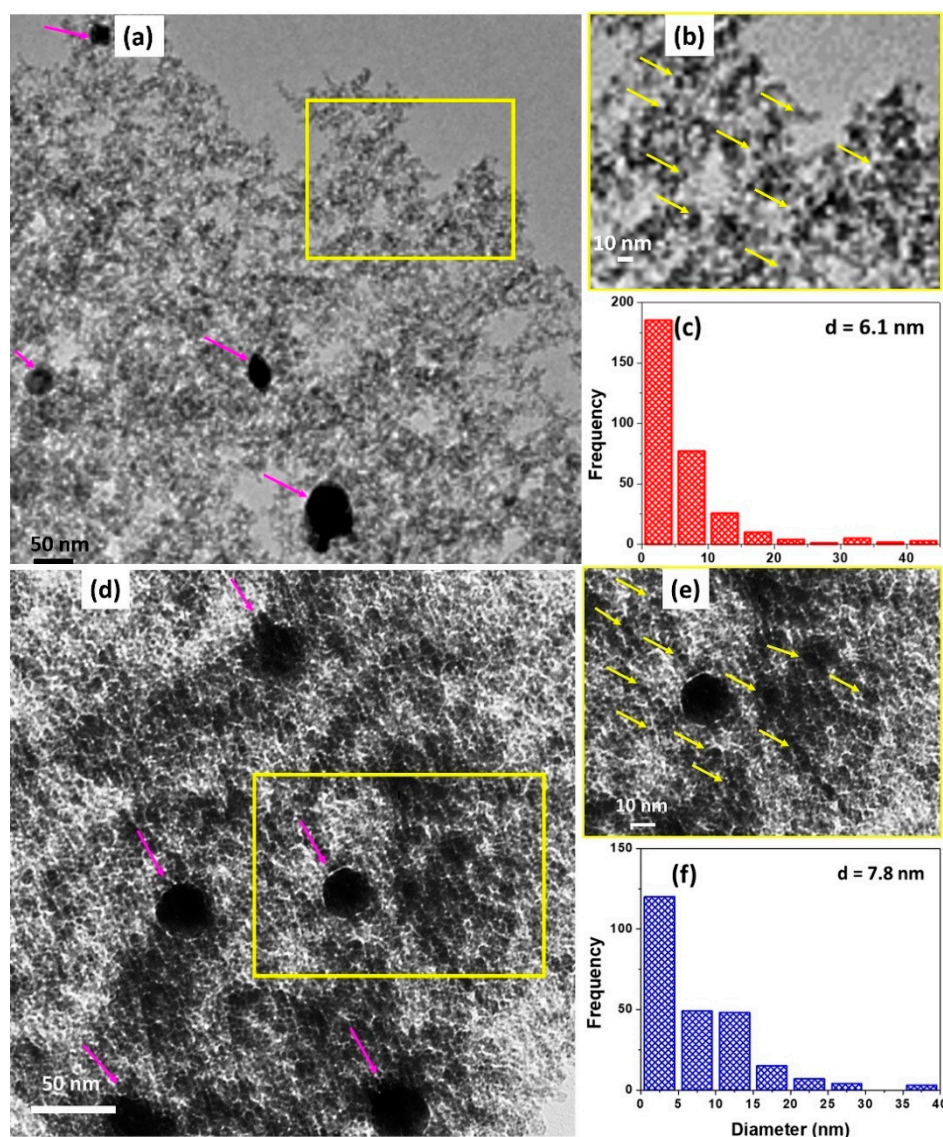


Figure 2. TEM micrographs and the corresponding estimated particle size distribution of Pd/SiO₂ aerogel catalysts (a–c) before, and (d–f) after the catalytic CO oxidation.

The XPS spectrum of the core level Pd 3d peaks were obtained from the samples at different points and verified by the NIST Standard XPS Database for PdO_x/Pd and Pd/SiO_x. The deconvolution of the spectrum of Pd 3d shows two spin-orbital states, 3d_{5/2} and 3d_{3/2} [2]. The Pd 3d and O 1s XPS peaks located in the near-surface region of freshly prepared Pd/SiO₂ samples, at 250 °C (full CO conversion), and after catalytic CO oxidation were investigated to understand the chemical environment, palladium oxidation state, and active species before and after the CO oxidation reaction. The Pd 3d showed peaks for Pd 3d_{5/2} and Pd 3d_{3/2} and fitted with the mixed Pd(0) and PdO combined spectrum. Table 3 summarizes the binding energies (BEs) of palladium Pd 3d_{5/2}, Pd 3d_{3/2}, and the binding energy (BE) of the corresponding O 1s peak [27]. The O 1s peak was fitted with three components due to the overlap of O 1s and Pd 3P3/2 peaks following Zemlyanove et al. [28]. Figure 3 shows Pd 3d and O 1s spectra of the reduced Pd/SiO₂ catalysts along with the deconvoluted peaks. Figure 3a shows Pd 3d spectra for the fresh (or as prepared) catalyst with two peaks at binding energies (BE) at 334.06 and 339.3 eV assigned to the metallic palladium Pd(0) and two peaks observed at 335.8 and 341 eV assigned to Pd²⁺ or PdO, respectively. This clearly indicates that most of Pd exists in the form of Pd metal with only a small fraction in the Pd²⁺ form. Upon increasing

the temperature to 250 °C (Figure 3b), the obtained spectrum of the sample shows that the low energy doublet of $3d_{5/2}$ is shifted to 335.1 eV which could be assigned to the photoemission of electrons from Pd^{2+} and the high energy doublet is shifted to 336.1 eV due to the oxidation of smaller Pd particles (2–3 nm) or Pd^{2+} cations within the catalyst structure [29]. The increase in BE of Pd 3d for the catalyst annealed at 250 °C affirms the increase in formation of PdO, indicating that the surface of Pd is highly oxidized. After the CO oxidation reaction (Figure 3c,f) the deconvolution of the Pd 3d peaks show Pd(0) and Pd^{2+} (PdO) peaks with higher concentration of PdO compared to freshly prepared samples.

Table 3. List of the binding energies of palladium species (Pd and PdO) and the binding energy of the corresponding O 1s peak located in the near-surface region of Pd/SiO₂ catalysts.

Catalyst	Binding Energy, eV		
	Pd $3d_{5/2}$	Pd $3d_{3/2}$	O 1s
Fresh	334.1	339.3	531.5
At 250 °C	335.13	340.23	531.6
After CO oxidation	334.8	339.9	531.8

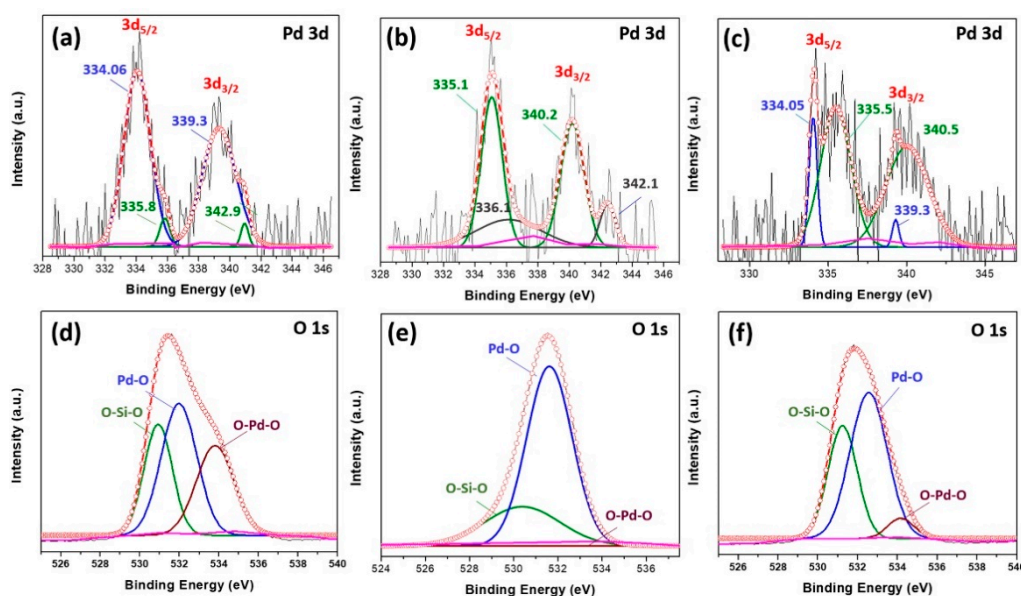


Figure 3. High-resolution XPS spectra of Pd 3d of (a) fresh Pd/SiO₂ catalysts, (b) Pd/SiO₂ catalysts annealed at 250 °C (full CO conversion), and (c) Pd/SiO₂ catalysts after the heating/cooling cycle in the CO/O₂ reaction mixture, and the deconvolution of O 1s XPS spectrum: (d) Before CO oxidation, (e) at 250 °C, and (f) after CO oxidation.

To analyze the change in the concentration of Pd^{2+} before and after CO oxidation, we compared the areas under the Pd $3d_{5/2}$ of Pd(0): Pd^{2+} peaks before CO oxidation (Figure 3a) to the ratio of areas of the peaks after CO oxidation (Figure 3c). The ratio of areas under the peaks of Pd(0): Pd^{2+} were 1.8:1 before and 1:1.6 after CO oxidation, respectively, indicating that the PdO concentration increases after CO oxidation, suggesting a lowering of the activation energy and confirming that the active phase for CO oxidation is PdO [29]. The increase in surface oxygen concentration (Pd-O) after the reaction (Figure 3f) could aid the activation of the C-O bond in the CO molecule for other oxidation reactions as reported elsewhere [23]. This increase is also accompanied by a reduction of oxygen concentration (O-Pd-O), which suggests that Pd interacts with the SiO₂ support [30,31]. Oxygen in SiO₂ loses electrons resulting in a shift and bending of the Fermi level. O₂ initially diffuses to the metallic Pd surface, where it is adsorbed to form an active adsorption state. Following this, the oxygen atoms interact with the Pd atoms on the surface to form PdO.

Results obtained from the XPS analysis show that the active sites and the state of Pd can provide valuable information on the metal-support interaction in the Pd/SiO₂ catalyst through monitoring of the electronic modifications of the Pd surface before and after the CO oxidation. This observation is consistent with the XRD [2] and TEM results. The XPS of the freshly prepared Pd/SiO₂ aerogel catalyst confirms that the Pd nanoparticles are attached to the support material through oxygen atoms of either the free silanol or siloxane groups present on the silica-network as oxygen is highly electronegative and can draw more electrons from Pd nanoparticles, resulting in higher BE for the Pd atoms in the Pd/SiO₂ catalyst.

2.1.2. Effect of Annealing Atmosphere on Catalytic Efficiency and Hysteresis of Pd/SiO₂ Aerogel Catalyst

The oxidation state of Pd alone cannot explain the change of the catalytic activity and hysteresis behavior before and after the heat treatment. To examine the thermal stability and catalytic performance of the catalyst aiming at optimizing the best condition for Pd active sites, we conducted several experiments to support our results. It has been reported that the catalyst support modification can contribute to the activity and hysteresis behavior of the catalyst due to its binding to the catalyst metal. This metal-support interaction modifies both the electronic and geometric properties of the catalyst support, which influences the activity of the catalytic sites on the metal surface and enhances active sites [23]. Reportedly, the hysteresis effect depended on the pretreatment of catalysts and was attributed to the changes in the catalyst structure for CO oxidation on partially oxidized Pd nanoparticles, where hysteresis effects were found to depend on the pretreatment of catalyst samples [32]. Pretreatment conditions of the catalyst influence the catalytic activity, and metal-support interaction motivated by the oxidation state of metal and the nature of the reactions. The effect of the catalyst pretreatment on the hysteresis behavior was reported and attributed to the changes in the catalyst structure [17]. Therefore, the pretreatment atmosphere is an essential factor that influences the final state of the catalyst and metal-support interaction. Oxidizing or reducing the atmosphere can yield oxide active or metallic phases depending on the temperature of the treatment.

The effect of the pretreatment atmosphere on catalytic activities, hysteresis, and ignition/extinction curves of Pd/SiO₂ aerogel catalyst was studied, and the results are summarized in Table 4 and Figure 4. The catalytic ignition/extinction curves and hysteresis of Pd/SiO₂ aerogel catalyst freshly prepared and annealed in different atmospheres have been plotted. It is clear that under ignition, the catalytic activities of annealed samples are higher, and the ignition temperatures are shifted to lower temperatures, which are attributed to the efficient removal of adsorbents from the surface, improving the exposure of active sites to fresh adsorbates possibly led by the decomposition of the metal complex to metal or metal oxide. However, the best activity and highest increase in the hysteresis width was observed for the sample treated in air. The results can be explained based on the gas composition of the annealing atmosphere, the reactant gas mixture, and the nature of gas used in the annealing atmosphere (reducing or oxidizing). Although, He and N₂ are inert gasses and do not affect the oxidation state of the freshly prepared Pd/SiO₂ aerogel catalyst, the thermal treatment at high temperature can affect the physio-chemical properties of the catalyst. The Pd/SiO₂-air aerogel sample showed the best catalytic activity compared to the untreated Pd/SiO₂ and Pd/SiO₂-N₂ aerogel samples, a plausible reason being that during the reaction, some of the metallic Pd nanoparticles converts to PdO as observed in XPS results, and the interfaces between Pd and PdO act as active catalytic sites. During extinction, the sample treated in N₂ gas shows an extinction temperature of 123 °C and hysteresis width of 104 °C, while the Pd/SiO₂-air aerogel sample, on the other hand, has an extinction temperature of 79 °C and a wider hysteresis width of 138 °C. This may arise from the formation of PdO in the Pd/SiO₂-air aerogel sample in the whole bulk of the catalyst during heating in the presence of excess O₂ through surface oxidation of metallic Pd preceded by diffusion of oxygen atoms from the bulk of the catalyst [33]. During extinction, the surface PdO is reduced directly to metallic Pd. The appearance of the

hysteresis loop can be associated with the slow transition from an oxygen-enriched surface and surface palladium oxide formation, present during extinction, to a CO-covered surface including Pd reduction, resulting in reversible formation of surface Pd oxide. Since Pd in the Pd/SiO₂-air aerogel sample was oxidized entirely, the reduction of Pd oxide will take a longer time than in the Pd/SiO₂ aerogel treated in N₂ samples, resulting in the broadening of the hysteresis curve [34].

Table 4. Catalytic ignition and extinction profile of Pd/SiO₂ aerogel catalysts annealed in different atmospheres.

Gas	T_{ig} (°C)	T_{50} (°C)	T_{100} (°C)	T_{ex} (°C)	Hysteresis Width (°C)
Untreated	214	276	296	138	121
Air	212	223	225	79	138
N ₂	212	248	287	123	104

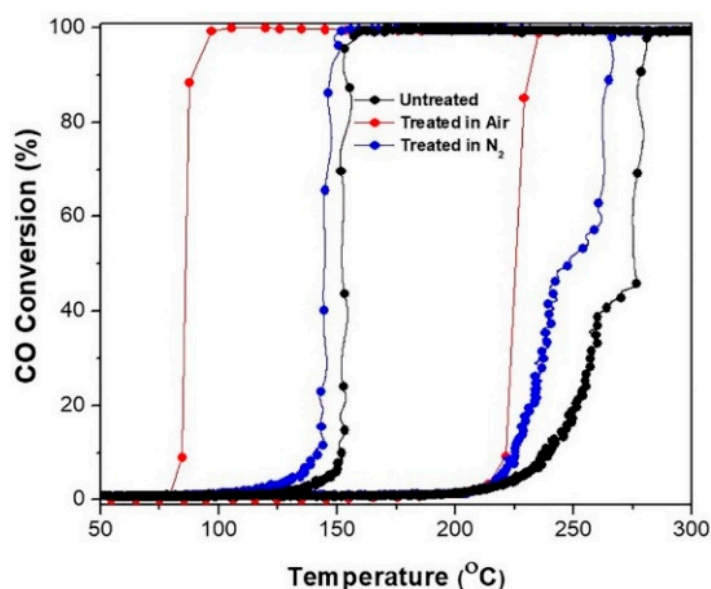


Figure 4. Comparison between the catalytic activity curves of Pd/SiO₂ aerogel catalysts annealed in different atmospheres during ignition and extinction.

To investigate the thermal stability of Pd/SiO₂ aerogel catalyst and the surface oxidation and reduction of Pd/SiO₂, TGA was performed up to 600 °C at a heating rate of 10 °C/min in air and N₂ atmospheres, while the DSC of Pd/SiO₂ aerogel was carried out under heating (red) and cooling (black) at a heating rate of 10 °C/min in air and N₂ atmospheres up to 300 °C, which corresponds to the temperature where full CO conversion is reached. TG-DSC spectra are shown in Figure 5. During heating, TGA and DSC studies for samples treated in an air environment showed two exothermic peaks and one endothermic peak, as shown in Figure 5a,c. The spectra indicate clearly that the catalyst is thermally stable up to 600 °C. A weight loss of ~3 wt% occurs when the samples are heated from 50 to 100 °C due to the loss of physically adsorbed water and ethanol from the porous catalyst.

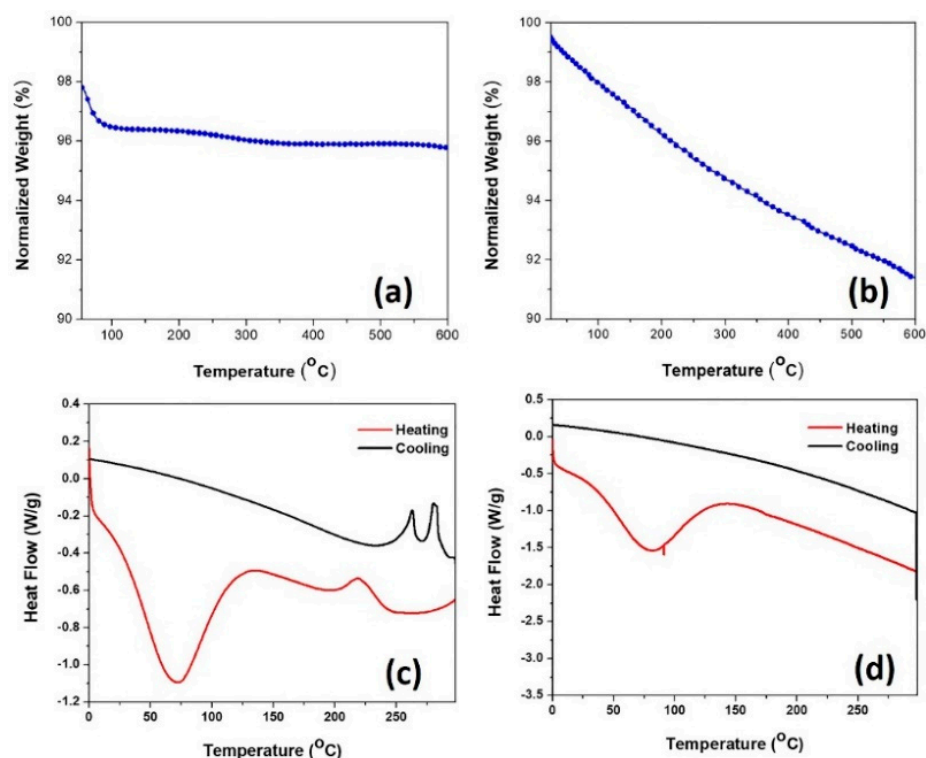


Figure 5. (a,c) Thermal gravimetric analysis-differential scanning calorimetry (TGA-DSC) of Pd/SiO₂ aerogel catalysts heated in the air atmosphere, (b,d) TGA-DSC of Pd/SiO₂ aerogel catalysts heated in the N₂ atmosphere.

These results are consistent with the DSC results, which show an endothermic peak in the region from room temperature up to 125 °C. Furthermore, an exothermic peak accompanied by an endothermic peak between 215 and 243 °C can be attributed to the surface oxidation of palladium accompanied with the reduction of silica surface, indicative of the formation of the interface between the palladium and silica support [35]. During the cooling ramp, as shown in Figure 5c, two exothermic peaks at 315 and 225 °C accompanied with an endothermic peak in between, could be attributed to the reduction of the small domain PdO to Pd⁰ on the surface of PdO, leading to polycrystalline particles that easily re-oxidize upon cooling due to the lack of Pd nucleation sites on the surface of the metal particles. Moreover, this could be associated with the combustion of unreacted organics such as Si-CH₃ groups from the synthesis process. This behavior was observed previously by Datye et al. on the surface of Pd/Al₂O₃ when the catalysts were heated in air [36] and Colussi et al. at higher temperature on Pd/Al₂O₃ and Pd/CeO₂/Al₂O₃, where they reported re-dispersion of Pd on the surface of oxide and transformation between Pd and PdO [37]. The temperature of this transformation was reported to strongly depend on the characteristics of the oxide support [38]. The results agree with the XPS analysis and catalytic tests of Pd/SiO₂ treated in air under heating/cooling cycles. However, TGA and DSC studies for samples treated in a nitrogen environment showed only well-resolved steps, Figure 5b,d. The major weight loss (about 5 wt%) was observed between 50 and 125 °C as evident in the DSC, as the broad endothermic peak in the curve in Figure 5d is attributed to the loss of water from the porous catalyst [39]. After 125 °C, the weight loss until 600 °C is attributed to the condensation of silanol groups from the surface of pristine silica aerogel, which was experimentally found to occur between 150 and 500 °C, as reported by Mueller et al. [40]. No peaks were observed during the cooling cycle which suggest that most of Pd in the sample is in the metallic state.

It is well known that the support nature and composition of SiO₂ and pretreatment conditions (oxidation or reduction treatments) have a direct impact on the metal-support

interaction and ratio of oxidized and reduced forms of the supported palladium metal. To investigate the thermal effect on the catalytic activities, hysteresis behavior, and surface oxidation and reduction of Pd/SiO₂ heated in air and N₂ atmospheres, we performed FTIR spectroscopy of Pd/SiO₂ aerogel catalyst annealed in different atmospheres (N₂ and air) and compared it to the untreated catalysts. Figure S2 compares FTIR spectra of freshly prepared Pd/SiO₂ aerogel catalysts and after the heat treatment at 450 °C in air and nitrogen atmospheres. Room-temperature FTIR spectra of Pd/SiO₂ samples measured in spectral range (400–4000 cm⁻¹) were recorded and compared to the untreated samples to determine the changes after annealing in N₂ and air atmospheres. The FTIR spectra of both samples revealed several sharp, well-defined absorption bands within the measured spectral range. The spectra show bands centered at 567, 794.5, and 1049.1 cm⁻¹ with a shoulder peak at 1162.9 cm⁻¹ corresponding to stretching vibrations of siloxane groups (Si–O–Si bonds), respectively [41], while the peak centered at 954.5 cm⁻¹ corresponds to the stretching vibration of silanol groups (Si–OH) in the silica lattice suggesting the presence of a considerable amount of silanol groups on the silica surface or pores in all the samples. A small peak observed at 2987.2 cm⁻¹ is assigned to the vibrations of the stretching vibration of –CH₃ and –CH₂ groups indicating the presence of a small amount of Si–OC₂H₅ groups, which can be attributed to an incomplete condensation during gelation [42]. The low-intensity peak at 3367.1 cm⁻¹ is assigned to –OH stretching vibrations [43].

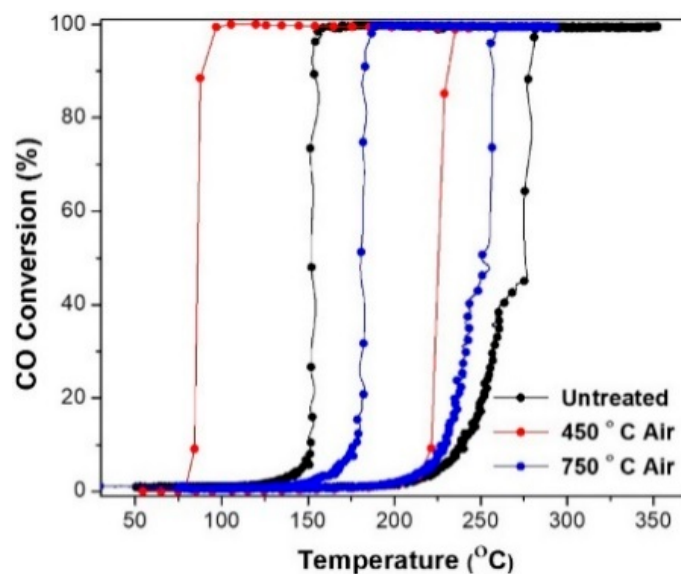
The FTIR spectra of the Pd/SiO₂ sample treated in air show that all peaks are shifted to a higher wavenumber compared to the untreated sample indicating the interaction between Pd and SiO₂, which can affect the formation of the Si–O–Si network as observed in Cu/SiO₂ [44] leading to a stronger metal-support interaction. The intensity of the peak at 958.45 cm⁻¹ is considerably lower, while that at 794.5 cm⁻¹ increases indicating the formation of new Si–O–Si bonds via the reduction of Si–OH bonds as a result of the condensation reaction between Si–O and the Pd metal. This reaction could shrink the SiO₂ network, which might be responsible for decreasing the pore volume and, consequently, surface area, as observed in N₂ adsorption-desorption results suggesting that the SiO₂ framework is formed by the Si–O–Si bonds [19]. Furthermore, the intensity of the peak at 3367.1 cm⁻¹, which is assigned to –OH stretching vibrations decreases, suggesting removal of the adsorbed OH or water. However, the FTIR spectra of Pd/SiO₂ sample treated in a nitrogen atmosphere showed similar spectra of the untreated sample (no shift is observed) except for reducing the intensity of the peak at 1162.9 cm⁻¹, which indicates the reduction of the Si–O–Si bond. The results suggest that the heat treatment in N₂ environment did not affect the interaction between Pd and the SiO₂ network.

2.1.3. Effect of Annealing Temperature on Catalytic Efficiency and Hysteresis of Pd/SiO₂ Aerogel Catalyst

A further impact of annealing temperature on the catalytic activity, hysteresis, and ignition/extinction of Pd/SiO₂ treated in the air aerogel catalyst was studied by annealing some samples at 450 and 750 °C in air as summarized in Table 5 and shown in Figure 6. During the ignition cycle, the air-annealed catalysts demonstrated higher activity compared to the freshly prepared catalysts mainly due to the removal of moisture and hydrocarbons from the surface of the catalyst and the reduction of metal oxide to metallic Pd and improving the active site for the CO oxidation reaction. The catalyst treated at 450 °C in air shows better activity than fresh catalysts due to the removal of silanol groups, which increases the metal dispersion and the catalytic activity of Pd/SiO₂ catalyst [21]. The results indicate that the heat treatment in air does not probably affect the Pd clusters or particles as they are pinned to the silica surface, and the diffusion of ions is difficult, preventing sintering. The Pd clusters showed resistance to sintering upon calcination to 550 °C in air, which was attributed to the confinement of Pd clusters within mesopores [45].

Table 5. Catalytic ignition and extinction profile of Pd/SiO₂ aerogel catalysts annealed in air for 1 h at different temperatures.

Annealing Temperature	T_{ig} (°C)	T_{50} (°C)	T_{100} (°C)	T_{ex} (°C)	Hysteresis Width (°C)
Untreated	214	276	296	138	121
450 °C Air	212	223	225	79	138
750 °C Air	214	251	259	157	70

**Figure 6.** Comparison between the catalytic activity curves of Pd/SiO₂ aerogel catalysts annealed for 1 h in air at different temperatures during ignition and extinction cycles.

The Pd/SiO₂-air aerogel catalyst initially contained a considerable amount of metal oxide; heating in air will ensure that the sample is fully oxidized at 450 °C. In studies on the catalytic activities conducted in the CO/O₂ mixture, PdO will undergo a reduction to Pd, which in-effect would prevent any Pd particle growth (due to sintering) up to 700 °C, except for outermost particles (outside the pores). Upon annealing at 750 °C, all PdO will be reduced to metallic Pd and this will lead to the growth and sintering of metallic Pd particles which would lower catalytic activity [46]. The presence of fully oxidized Pd particles and well-defined active sites in the samples annealed at 450 °C in air ensures higher activity and lower extinction temperature. The as-prepared samples contain a considerable amount of metallic Pd, and most of the active sites are blocked, making it less active even during extinction. For samples annealed at 750 °C, the growth and sintering of the Pd particles lead to a lower activity resulting in narrower hysteresis width and lower ignition temperature compared to the sample treated at 450 °C.

Based on the experimental results, the origin of the high thermal stability and catalytic performance of Pd/SiO₂ aerogel catalysts were attributed to their mesoporous structures as confirmed by the N₂ adsorption-desorption isotherm, XPS, FTIR, and TEM. The results also confirmed that the catalyst structure could protect the Pd nanoparticles from sintering during the thermal treatment and catalytic CO oxidation reaction. The thermal stability of the Pd/SiO₂ catalyst highly depends on the oxidative/reductive nature of the gas environment. Under the CO oxidation reaction in the oxygen atmosphere, a small amount of Pd is converted to PdO. However, under air atmosphere, the porous structure of the silica is still stable, and the formation of small Pd particles inside the SiO₂ pores and on the surface increases as temperature increases.

Moreover, the absence of reducing gases in air leads to the oxidation of Pd particles, which directly impacts thermal stability and catalyst performance. The same behavior

was observed under air and H₂ environment [47]. The FTIR results confirmed that the interaction of Pd sites with -OH on the SiO₂ stabilizes the catalyst surface resulting in excellent thermal stability. Consequently, the Pd/SiO₂ catalysts showed a much more stable CO oxidation performance after annealing in air. These results agree well with recent studies, suggesting that the thermal treatment by annealing and catalytic CO oxidation at high temperatures (below 500) enhances the stability of Pd/SiO₂ catalyst under catalytic CO oxidation reactions due to its structure stability [48].

To understand the effect of annealing temperature on the catalytic activities, hysteresis behavior, and surface oxidation and reduction of Pd/SiO₂ catalyst heated in air atmosphere at different temperatures. We performed FTIR spectroscopy of Pd/SiO₂ aerogel catalyst annealed at 450 and 750 °C in air atmospheres than the untreated catalyst. Figure S3 shows FTIR spectra of the freshly prepared Pd/SiO₂ aerogel catalyst and after the heat treatment at 450 and 750 °C in air, respectively. The infrared absorption is similar to the discussion mentioned above in Figure S2 with bands centered at 567, 794.5, and 1049.1 cm⁻¹ with a shoulder at 1162.9 cm⁻¹ corresponding to stretching vibrations of siloxane groups (Si-O-Si bonds), respectively. A peak centered at 954.5 cm⁻¹ corresponds to the stretching vibration of silanol groups (Si-OH) in the silica lattice which suggest the presence of a considerable amount of silanol groups on the silica surface or the pores in all samples. Small peaks observed at 2987.2 and 3367.1 cm⁻¹ are assigned to the stretching vibration of -CH₃ and -CH₂ to -OH stretching vibrations or water, as reported earlier. As the annealing temperature increases, the peak at 958.45 cm⁻¹ slowly disappears, the intensity of the peak at 2987.2 cm⁻¹ decreases, while that of the peak at 794.5 cm⁻¹ increases. This suggests the formation of additional Si-O-Si bonds by the condensation reaction. The peaks at 1710 and 3367.1 cm⁻¹ that belong to vibrations of water molecules decrease with the increasing annealing temperature due to the removal of water from the SiO₂ network structure [23]. The results suggest that heating to 750 °C could lead to the formation of additional Si-O-Si bonds, which strengthens the SiO₂ network structure [19]. The presence of 958.45 cm⁻¹, which corresponds to the stretching vibration of silanol groups (Si-OH) in the sample heated at 450 °C, enhanced the Pd-silica interaction, facilitating the dispersion of Pd particles.

2.2. Hysteresis Behavior during (Ignition/Extinction) Cycles

The reaction mechanism of CO oxidation during ignition/extinction cycles was reported by many researchers. CO is strongly adsorbed onto Pd, inhibiting the formation of active oxygen needed for low-temperature CO oxidation. Hence, low-temperature CO oxidation over Pd catalysts proceeds via Langmuir-Hinshelwood. Such adsorption has been shown to occur during CO oxidation on Pd metal catalysts under low O₂ pressure, wherein CO and O₂ gas are adsorbed on free adsorption sites on the Pd metal surface, followed by the interaction of the adsorbed CO and O, respectively, on the Pd active sites, resulting in the palladium oxide (PdO) surface. However, the reduction of PdO proceeds via the Mars-van Krevelen mechanism, where CO is adsorbed on the PdO surface [49].

The TEM results of large surface particles in the Pd/SiO₂ catalyst suggest that the as prepared catalyst contains Pd particles and a small amount of PdO particles on the surface, as shown in Figure 7a, while at 250 °C, the surface is almost fully covered with oxide as shown in Figure 7b, suggesting the formation of surface and bulk oxides. The TEM image of the particles after the heating/cooling cycle (Figure 7c) shows that part of the Pd (0) surface is restored, and the PdO surface is destroyed with a small island of 2D PdO observed. Similar observations in the literature suggested the oxidation of Pd and the formation of surface oxide during heating [12]. At higher temperatures, wherein the formation of 3D PdO is preferential on the catalyst surface while during cooling conditions, the 3D PdO is reduced to the Pd surface. The TEM results agree well with the XPS peak fitting, which show a shift of Pd 3d_{5/2} peak towards higher BE (Figure 3b) with respect to the metal peak (Figure 3a) due to the interaction with atomic oxygen to form PdO during the CO oxidation reaction. However, during cooling to room temperature (after heating/cooling

cycle) and as a result of the reaction medium (Figure 3c), PdO particles are reduced, leading to a decrease in the oxide intensity. In this region, the metallic palladium Pd(0) and the PdO particles co-exist, which serve as intermediates causing the self-sustained oscillation and hysteresis. A similar behavior was reported for Pd/Al₂O₃ systems [12].

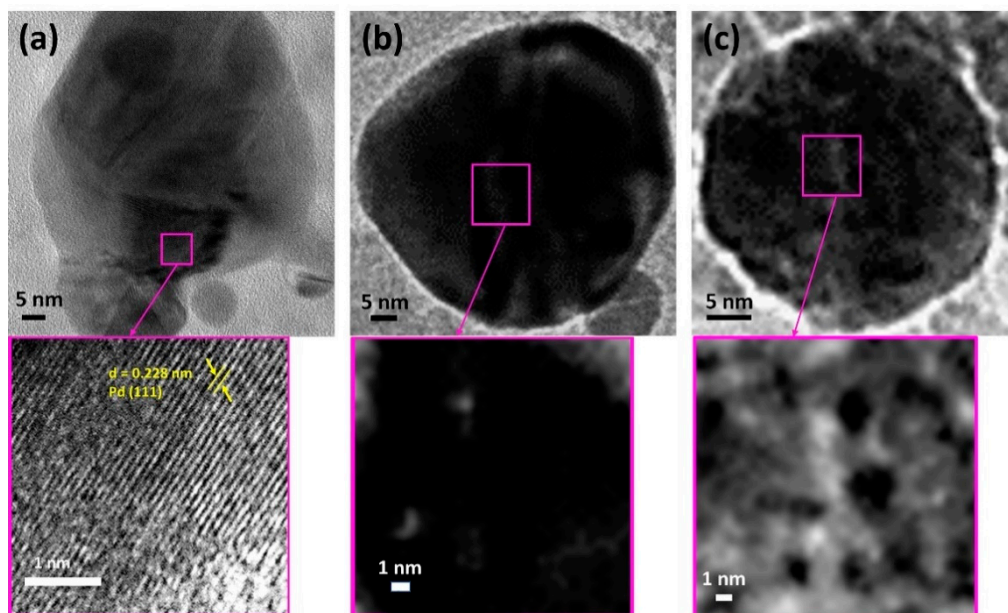


Figure 7. TEM of (a) the fresh Pd/SiO₂ catalysts, (b) Pd/SiO₂ catalysts annealed at 250 °C in air, and (c) after heating/cooling cycle in the CO/O₂ reaction mixture.

In our study, XPS and TEM results suggest that the oxidation state, morphology of the Pd/SiO₂ catalyst, and the large palladium surface particles, changed before, during, and after the CO oxidation reaction. The presence of surface and subsurface Pd (0) and PdO with 2D morphologies, and the interplay between the two phases (reversed oxidation of Pd (0) and reduction or decomposition of PdO) causes the oscillatory behavior and hysteresis during the CO oxidation reaction, which aid the catalytic activity by lowering the activation energy after the first light-off.

3. Experimental Methodology

3.1. Catalyst Synthesis

The catalysts were prepared using the sol-gel method and dried under conditions with supercritical ethanol at 260 °C. This synthesis method described in a previous study [26] ensured the synthesis of well-dispersed Pd nanoparticles on a silica support. The silica gel was impregnated with metal ions before the drying step to replace the pores previously filled with the solvents used in the synthesis, which leads to hierarchical porosity. The advantage of this synthesis method is the possibility of producing highly dispersed and stable Pd catalysts with controlled structures and catalytic performances. The resulting Pd/SiO₂ catalyst is composed of accessible palladium particles located inside the pores or within the network silica particles, which result in sinter-proof Pd particles. The active catalytic sites are easily accessed by the reactants by diffusing through micropores and mesopores with no mass transfer limitations [23].

In a typical synthesis with tetraethyl orthosilicate (TEOS, Sigma-Aldrich, St. Louis, MO, USA, 98%) and ethanol, the resultant solution is aged overnight in a sealed container to obtain a gel [18]. The wet-gel obtained is then transferred to a solution of palladium precursor (PdCl₂, Sigma-Aldrich, St. Louis, MO, USA) in ethanol. The silica aerogels are dipped in the solutions of Pd ions in ethanol to ensure the exchange of ethanol in the gel with the Pd ions in the solution, followed by the ethanol supercritical drying at

260 °C. Dried Pd supported silica aerogels were annealed at a heating rate of 10 °C under atmospheric pressure (1 atm) in two different ambient conditions: Air (Pd/SiO₂–air), nitrogen (Pd/SiO₂–N₂), each at a 100 mL/min flow rate. All catalytic experiments and characterization were carried out using powdered aerogels.

3.2. Catalysts Characterization

The Pd/SiO₂ aerogel catalysts were characterized by X-ray photoelectron spectroscopy (XPS; Omicron Nanotechnology, Germany) with a monochromatic Al K_α radiation (energy = 1486.6 eV) working at 15 kV, which was used to study the surface states of the catalyst. The obtained XPS spectra were calibrated with respect to the C 1s feature at 285 eV [49]. The catalyst's surface area and pore sizes were determined using a Rise 1010 surface area and porosity analyzer (Jinan Rise Science and Technology Co., Ltd., Jinan, China). The Brunauer–Emmett–Teller (BET) and Langmuir models based specific surface area were calculated from the nitrogen adsorption-desorption isotherms recorded at 77 K at the relative pressure range of P/P₀ = 0.05–0.2. Pore size distributions were calculated using the desorption branches of the isotherms using the Barrett–Joyner–Halenda (BJH) model [50]. Transmission electron microscopy (TEM) measurements were carried out using a (JEM2100F field emission transmission electron microscope (TEM)) operating at a voltage of 200 kV (JEOL Ltd., Tokyo, Japan). Fourier transform infrared (FTIR) spectroscopy was performed using the FTIR650 spectrometer equipped with a LA-025-1100 universal ATR unit (Labfreez Instruments (Hunan) Co., Ltd., Changsha, China). Thermogravimetric analysis (TGA) and differential scanning calorimetry (DSC) were performed using the TG 2100D (Analytical Technologies Limited, Shanghai, China) analyzer at a ramp rate of 10 °C/min to reach (from 23 to 800 °C) in air (flow rate of 100 cc/min).

3.3. Catalyst Activity Testing

Catalytic activities of the synthesized samples were carried out in a custom-built fixed-bed continuous flow reactor placed inside a programmable tube furnace coupled to an infrared gas analyzer (ACS-CO₂ infrared analyzer) [2]. Twenty milligrams of powdered metal loaded aerogel catalyst was placed in the middle of a quartz tube and sandwiched between two pieces of glass wool to form a cylindrical pellet. The catalyst temperature was recorded using an Omega K-type thermocouple inserted in the middle of the sample. The reactant gas mixture containing 3.5 wt% CO and 20 wt% O₂ in helium was flown through the reactor at 100 mL/min (calculated weight hourly space velocity (WHSV) was approximately 300,000 mL g⁻¹h⁻¹). CO conversion was assessed by measuring CO₂ in the outflow with an IR analyzer, and the catalytic activity was expressed by the CO conversion in the effluent gas. The temperature and the concentration data were collected using a National Instruments multifunction USB-6008 and NI-DAQmx (National Instruments, Roscoe, IL, USA) data acquisition system and recorded using a custom-built LabVIEW data acquisition software. The gas flow rate was controlled by a set of digital mass flow controllers. The flow rate of the mixture was maintained at 100 mL/min, while the catalyst was heated to different temperatures (25–600 °C). All the experiments were performed at an atmospheric pressure (1 atm) with a heating rate of 10 °C/min (ignition or activation) until the CO conversion reaches a full conversion (100%), then the furnace was switched off, and the sample was left to cool naturally until the CO conversion became zero (0%) (extinction or relaxation). Catalyst conditioning was achieved by calcination of the catalyst at 450 °C in air atmosphere for 1 h. For the other experiments, the calcination temperature was changed to 750 °C in air or N₂ for 1 h. The process is capable of removing moisture and improving the active sites. The ignition/light-off and extinction/light-out temperatures denoted the temperatures where the CO conversion reaches 3% during ignition and extinction curves. The CO conversion of the catalyst was measured as a function of the catalyst temperature and calculated using the following relation:

$$\text{CO conversion (\%)} = \frac{[\text{CO}]_{\text{in}} \text{vol.\%} - [\text{CO}]_{\text{out}} \text{vol.\%}}{[\text{CO}]_{\text{in}} \text{vol.\%}} \times 100 \quad (1)$$

where $[\text{CO}]_{\text{in}}$ is the CO concentration in the reaction gas mixture and $[\text{CO}]_{\text{out}}$ is the concentration in the product gas mixture.

4. Conclusions

In this work, the low temperature CO oxidation and hysteresis behavior as a function of the catalyst temperature under optimum reaction conditions was investigated over a range of pretreatment mixture/conditions and temperatures that directly affect the nature of the active site. Carefully designed control experiments provide strong evidence that the pretreatment temperature and medium, nature of the support (porosity, thermal conductivity), the stability of the active site, and their formation were crucial factors in enhancing the catalytic performance. The best low-temperature CO oxidation performance was achieved by pretreating the catalyst in an air atmosphere at 450 °C. Recent studies suggest that the catalyst activation and the CO conversion hysteresis is attributed to local heating and heat dissipation by the support, respectively. However, the results presented here suggest that pretreatment conditions in N₂ or air, and the pretreatment temperature have a direct impact on the catalyst activation and hysteresis behavior, in addition to the structural and chemical effect of the catalyst. The active site formation is influenced by the presence of oxidative or reductive pretreatment gas, and the surface morphological and chemical changes of the Pd during the reaction due to CO and O₂ adsorption to achieve the lower activation energy. Therefore, the hysteresis arises from the stabilization of these active sites by forming different oxidation states of Pd during the ignition and alteration of PdO to Pd during the extinction. These results were realized by the XPS, which suggest partial oxidation of Pd and the formation of different surface oxides reaching full oxidation at 250 °C. These results were confirmed by TEM, which show the formation and reduction of PdO during heating/cooling cycles. The TGA and DSC results confirm the surface oxidation and reduction behavior of Pd/SiO₂ in air for both the ignition and extinction cycles. Furthermore, the catalyst structure including the particle size distribution, the porosity of the sample, and thermal stability contribute to the catalytic activity and hysteresis phenomenon. This study confirms that the structure-activity relationship is very crucial for the design of a highly active and thermally stable catalyst for CO oxidation as a model reaction, which could aid the design of next-generation catalysts for CO oxidation.

Supplementary Materials: The following are available online at <https://www.mdpi.com/2073-4344/11/1/131/s1>. Figure S1: Langmuir isotherms of N₂ adsorption and desorption (a) and pore diameter distribution (b) of fresh Pd/SiO₂ aerogel catalysts before and after the catalytic CO oxidation (first light-off); Figure S2: Comparison between FTIR spectra of fresh Pd/SiO₂ aerogel catalysts and after the heat treatment at 450 °C in the air and nitrogen atmosphere; Figure S3: Comparison between FTIR spectra of fresh Pd/SiO₂ aerogel catalysts and after the heat treatment at 450 and 750 °C in air.

Author Contributions: R.M.A.S. synthesized materials, performed experiments and characterization, analyzed data, wrote and edited the entire paper; J.D. supervised the work and the quality of the manuscript; K.M.S. participated in characterization and data analysis; M.T.Z.M. and M.A.G. performed and analyzed XPS data. The authors worked together to prepare this manuscript. All authors have read and agreed to the published version of the manuscript.

Funding: We would like to acknowledge partial financial support from Swedish Energy Agency (Energimyndigheten) through a project entitled HESAC (Project No. 45504–1).

Institutional Review Board Statement: Not applicable.

Informed Consent Statement: Not applicable.

Data Availability Statement: Data is contained within the article.

Acknowledgments: We want to show our gratitude to Shaukat Saeed from the Pakistan Institute of Engineering and Applied Sciences (PIEAS), Islamabad, Pakistan, Ayman Samara from the Qatar Environment and Energy Research Institute (QEERI), Hamad Ben Khalifa University, Doha, Qatar, and Karthik Laxman Kunjali from the Royal Institute of Technology (KTH), Stockholm, Sweden who provided insights and expertise that helped our research.

Conflicts of Interest: The authors declare no conflict of interest.

References

1. Freund, H.J.; Meijer, G.; Scheffler, M.; Schlögl, R.; Wolf, M. CO Oxidation as a Prototypical Reaction for Heterogeneous Processes. *Angew. Chem. Int. Ed.* **2011**, *50*, 10064. [[CrossRef](#)] [[PubMed](#)]
2. Al Soubaihi, R.M.; Saoud, K.M.; Ye, F.; Zar Myint, M.T.; Saeed, S.; Dutta, J. Synthesis of hierarchically porous silica aerogel supported Palladium catalyst for low-temperature CO oxidation under ignition/extinction conditions. *Microporous Mesoporous Mater.* **2020**, *292*, 109758. [[CrossRef](#)]
3. Berlowitz, P.J.; Peden, C.H.F.; Goodman, D.W. Kinetics of carbon monoxide oxidation on single-crystal palladium, platinum, and iridium. *J. Phys. Chem.* **1988**, *92*, 5213–5221. [[CrossRef](#)]
4. Sawisai, R.; Wanchanthuek, R.; Radchatawedchakoon, W.; Sakee, U. Synthesis, Characterization, and Catalytic Activity of Pd(II) Salen-Functionalized Mesoporous Silica. *J. Chem.* **2017**, *2017*, 1–12. [[CrossRef](#)]
5. Kumar, S.; Boro, J.C.; Ray, D.; Mukherjee, A.; Dutta, J. Bionanocomposite films of agar incorporated with ZnO nanoparticles as an active packaging material for shelf life extension of green grape. *Heliyon* **2019**, *5*, e01867. [[CrossRef](#)]
6. Forman, A.J.; Park, J.-N.; Tang, W.; Hu, Y.-S.; Stucky, G.D.; McFarland, E.W. Silica-Encapsulated Pd Nanoparticles as a Regenerable and Sintering-Resistant Catalyst. *ChemCatChem* **2010**, *2*, 1318–1324. [[CrossRef](#)]
7. Min, B.K.; Santra, A.K.; Goodman, D.W. Understanding Silica-Supported Metal Catalysts: Pd/Silica as a Case Study. *ChemInform* **2004**, *35*. [[CrossRef](#)]
8. Gustafsson, T.; Garfunkel, E.; Gusev, E.P.; HÄBerle, P.; Lu, H.C.; Zhou, J.B. Structural studies of oxide surfaces. *Surf. Rev. Lett.* **1996**, *3*, 1561–1565. [[CrossRef](#)]
9. Chen, Z.P.; Wang, S.; Ding, Y.; Zhang, L.; Lv, L.R.; Wang, M.Z.; Wang, S.D. Pd catalysts supported on Co₃O₄ with the specified morphologies in CO and CH₄ oxidation. *Appl. Catal. A Gen.* **2017**, *532*, 95–104. [[CrossRef](#)]
10. Slavinskaya, E.M.; Stonkus, O.A.; Gulyaev, R.V.; Ivanova, A.S.; Zaikovskii, V.I.; Kuznetsov, P.A.; Boronin, A.I. Structural and chemical states of palladium in Pd/Al₂O₃ catalysts under self-sustained oscillations in reaction of CO oxidation. *Appl. Catal. A Gen.* **2011**, *401*, 83–97. [[CrossRef](#)]
11. Imbihl, R.; Ertl, G. Oscillatory Kinetics in Heterogeneous Catalysis. *Chem. Rev.* **1995**, *95*, 697–733. [[CrossRef](#)]
12. Lashina, E.A.; Slavinskaya, E.M.; Chumakova, N.A.; Stadnichenko, A.I.; Salanov, A.N.; Chumakov, G.A.; Boronin, A.I. Inverse temperature hysteresis and self-sustained oscillations in CO oxidation over Pd at elevated pressures of reaction mixture: Experiment and mathematical modeling. *Chem. Eng. Sci.* **2020**, *212*, 115312. [[CrossRef](#)]
13. Dadi, R.K.; Luss, D.; Balakotaiah, V. Dynamic hysteresis in monolith reactors and hysteresis effects during co-oxidation of CO and C₂H₆. *Chem. Eng. J.* **2016**, *297*, 325–340. [[CrossRef](#)]
14. Assovskii, I.G. Ignition, extinction, and thermal hysteresis of a heterogeneous exothermic reaction. *Combust. Explos. Shock Waves* **1998**, *34*, 163–169. [[CrossRef](#)]
15. Abedi, A.; Hayes, R.; Votsmeier, M.; Epling, W.S. Inverse Hysteresis Phenomena During CO and C₃H₆ Oxidation over a Pt/Al₂O₃ Catalyst. *Catal. Lett.* **2012**, *142*, 930–935. [[CrossRef](#)]
16. An, W.; Liu, P. The complex behavior of the Pd-7 cluster supported on TiO₂(110) during CO oxidation: Adsorbate-driven promoting effect. *Phys. Chem. Chem. Phys.* **2016**, *18*, 30899–30902. [[CrossRef](#)]
17. Koutoufaris, I.; Koltsakis, G. Heat- and mass-transfer induced hysteresis effects during catalyst light-off testing. *Can. J. Chem. Eng.* **2014**, *92*, 1561–1569. [[CrossRef](#)]
18. Al Soubaihi, R.; Saoud, K.; Dutta, J. Critical Review of Low-Temperature CO Oxidation and Hysteresis Phenomenon on Heterogeneous Catalysts. *Catalysts* **2018**, *8*, 660. [[CrossRef](#)]
19. Casapu, M.; Fischer, A.; Gänzler, A.M.; Popescu, R.; Crone, M.; Gerthsen, D.; Türk, M.; Grunwaldt, J.-D. Origin of the Normal and Inverse Hysteresis Behavior during CO Oxidation over Pt/Al₂O₃. *ACS Catal.* **2016**, *7*, 343–355. [[CrossRef](#)]
20. Daniell, W.; Landes, H.; Fouad, N.E.; Knözinger, H. Influence of pretreatment atmosphere on the nature of silica-supported Pd generated via decomposition of Pd(acac)₂: An FTIR spectroscopic study of adsorbed CO. *J. Mol. Catal. A Chem.* **2002**, *178*, 211–218. [[CrossRef](#)]
21. Kwon, J.S.; Kim, J.S.; Lee, H.S.; Lee, M.S. Surface Modification of SiO₂ for Highly Dispersed Pd/SiO₂ Catalyst. *J. Nanosci. Nanotechnol.* **2019**, *19*, 882–887. [[CrossRef](#)] [[PubMed](#)]
22. Panpranot, J.; Pattamakomsan, K.; Goodwin, J.G.; Praserttham, P. A comparative study of Pd/SiO₂ and Pd/MCM-41 catalysts in liquid-phase hydrogenation. *Catal. Commun.* **2004**, *5*, 583–590. [[CrossRef](#)]
23. Raj, R.; Harold, M.P.; Balakotaiah, V. Steady-state and dynamic hysteresis effects during lean co-oxidation of CO and C₃H₆ over Pt/Al₂O₃ monolithic catalyst. *Chem. Eng. J.* **2015**, *281*, 322–333. [[CrossRef](#)]
24. Inoue, S.; Hanzawa, Y.; Kaneko, K. Prediction of Hysteresis Disappearance in the Adsorption Isotherm of N₂ on Regular Mesoporous Silica. *Langmuir* **1998**, *14*, 3079–3081. [[CrossRef](#)]
25. Gage, S.H.; Engelhardt, J.; Menart, M.J.; Ngo, C.; Leong, G.J.; Ji, Y.; Trewyn, B.G.; Pylypenko, S.; Richards, R.M. Palladium Intercalated into the Walls of Mesoporous Silica as Robust and Regenerable Catalysts for Hydrodeoxygenation of Phenolic Compounds. *ACS Omega* **2018**, *3*, 7681–7691. [[CrossRef](#)]

26. Heinrichs, B.; Lambert, S.; Alié, C.; Pirard, J.P.; Beketov, G.; Nehasil, V.; Kruse, N. Cogelation: An effective sol-gel method to produce sinter-proof finely dispersed metal catalysts supported on highly porous oxides. In *Studies in Surface Science and Catalysis*; Gaigneaux, E., De Vos, D.E., Grange, P., Jacobs, P.A., Martens, J.A., Ruiz, P., Poncelet, G., Eds.; Elsevier: Amsterdam, The Netherlands, 2000; Volume 143, pp. 25–33.
27. Qi, T.; Sun, J.; Yang, X.; Yan, F.; Zuo, J. Effects of Chemical State of the Pd Species on H₂ Sensing Characteristics of PdO_x/SnO₂ Based Chemiresistive Sensors. *Sensors* **2019**, *19*, 3131. [[CrossRef](#)]
28. Zemlyanov, D.; Aszalos-Kiss, B.; Kleimenov, E.; Teschner, D.; Zafeiratos, S.; Hävecker, M.; Knop-Gericke, A.; Schlögl, R.; Gabasch, H.; Unterberger, W.; et al. In situ XPS study of Pd(111) oxidation. Part 1: 2D oxide formation in 10–3mbar O₂. *Surf. Sci.* **2006**, *600*, 983–994. [[CrossRef](#)]
29. Wang, Z.; Li, B.; Chen, M.; Weng, W.; Wan, H. Size and support effects for CO oxidation on supported Pd catalysts. *Sci. China Chem.* **2010**, *53*, 2047–2056. [[CrossRef](#)]
30. Juszczyk, W.; Karpiński, Z.; Łomot, D.; Pielaszek, J. Transformation of Pd/SiO₂ into palladium silicide during reduction at 450 and 500 °C. *J. Catal.* **2003**, *220*, 299–308. [[CrossRef](#)]
31. Riley, J.D.; Ley, L.; Azoulay, J.; Terakura, K. Partial densities of states in amorphousPd_{0.81}Si_{0.19}. *Phys. Rev. B* **1979**, *20*, 776–783. [[CrossRef](#)]
32. Dubbe, H.; Bühner, F.; Eigenberger, G.; Nieken, U. Hysteresis Phenomena on Platinum and Palladium-based Diesel Oxidation Catalysts (DOCs). *Emiss. Control Sci. Technol.* **2016**, *2*, 137–144. [[CrossRef](#)]
33. Shipilin, M.; Gustafson, J.; Zhang, C.; Merte, L.R.; Stierle, A.; Hejral, U.; Ruett, U.; Gutowski, O.; Skoglundh, M.; Carlsson, P.-A.; et al. Transient Structures of PdO during CO Oxidation over Pd(100). *J. Phys. Chem. C* **2015**, *119*, 15469–15476. [[CrossRef](#)]
34. Bychkov, V.Y.; Tulenin, Y.P.; Slinko, M.M.; Khudorozhkov, A.K.; Bukhtiyarov, V.I.; Sokolov, S.; Korchak, V.N. Self-oscillations during methane oxidation over Pd/Al₂O₃: Variations of Pd oxidation state and their effect on Pd catalytic activity. *Appl. Catal. A Gen.* **2016**, *522*, 40–44. [[CrossRef](#)]
35. Newton, M.A.; Belver-Coldeira, C.; Martínez-Arias, A.; Fernández-García, M. “Oxidationless” Promotion of Rapid Palladium Redispersion by Oxygen during Redox CO/(NO+O₂) Cycling. *Angew. Chem.* **2007**, *119*, 8783–8785. [[CrossRef](#)]
36. Datye, A.K.; Bravo, J.; Nelson, T.R.; Atanasova, P.; Lyubovsky, M.; Pfefferle, L. Catalyst microstructure and methane oxidation reactivity during the Pd↔PdO transformation on alumina supports. *Appl. Catal. A Gen.* **2000**, *198*, 179–196. [[CrossRef](#)]
37. Colussi, S.; Trovarelli, A.; Vesselli, E.; Baraldi, A.; Comelli, G.; Groppi, G.; Llorca, J. Structure and morphology of Pd/Al₂O₃ and Pd/CeO₂/Al₂O₃ combustion catalysts in Pd–PdO transformation hysteresis. *Appl. Catal. A Gen.* **2010**, *390*, 1–10. [[CrossRef](#)]
38. Yue, B.; Zhou, R.; Wang, Y.; Zheng, X. Study of the methane combustion and TPR/TPO properties of Pd/Ce–Zr–M/Al₂O₃ catalysts with M=Mg, Ca, Sr, Ba. *J. Mol. Catal. A Chem.* **2005**, *238*, 241–249. [[CrossRef](#)]
39. Zhuravlev, L.T. The surface chemistry of amorphous silica. Zhuravlev model. *Colloids Surf. A Physicochem. Eng. Asp.* **2000**, *173*, 1–38. [[CrossRef](#)]
40. Mueller, R.; Kammler, H.K.; Wegner, K.; Pratsinis, S.E. OH Surface Density of SiO₂ and TiO₂ by Thermogravimetric Analysis. *Langmuir* **2003**, *19*, 160–165. [[CrossRef](#)]
41. Bertoluzza, A.; Fagnano, C.; Antonietta Morelli, M.; Gottardi, V.; Guglielmi, M. Raman and infrared spectra on silica gel evolving toward glass. *J. Non-Cryst. Solids* **1982**, *48*, 117–128. [[CrossRef](#)]
42. Lamber, R.; Jaeger, N.; Schulz-Ekloff, G. Metal-support interaction in the Pd/SiO₂ system: Influence of the support pretreatment. *J. Catal.* **1990**, *123*, 285–297. [[CrossRef](#)]
43. Shewale, P.M.; Venkateswara Rao, A.; Parvathy Rao, A.; Bhagat, S.D. Synthesis of transparent silica aerogels with low density and better hydrophobicity by controlled sol–gel route and subsequent atmospheric pressure drying. *J. Sol-Gel Sci. Technol.* **2009**, *49*, 285–292. [[CrossRef](#)]
44. Li, G.; Zhu, T.; Deng, Z.; Zhang, Y.; Jiao, F.; Zheng, H. Preparation of Cu-SiO₂ composite aerogel by ambient drying and the influence of synthesizing conditions on the structure of the aerogel. *Chin. Sci. Bull.* **2011**, *56*, 685–690. [[CrossRef](#)]
45. Yuranov, I.; Moeckli, P.; Suvorova, E.; Buffat, P.; Kiwi-Minsker, L.; Renken, A. Pd/SiO₂ catalysts: Synthesis of Pd nanoparticles with the controlled size in mesoporous silicas. *J. Mol. Catal. A Chem.* **2003**, *192*, 239–251. [[CrossRef](#)]
46. Grunwaldt, J.-D.; Vegten, N.v.; Baiker, A. Insight into the structure of supported palladium catalysts during the total oxidation of methane. *Chem. Commun.* **2007**, 4635. [[CrossRef](#)]
47. Baaziz, W.; Bahri, M.; Gay, A.S.; Chaumonnot, A.; Uzio, D.; Valette, S.; Hirlimann, C.; Ersen, O. Thermal behavior of Pd@SiO₂ nanostructures in various gas environments: A combined 3D and in situ TEM approach. *Nanoscale* **2018**, *10*, 20178–20188. [[CrossRef](#)]
48. Hu, Y.; Tao, K.; Wu, C.; Zhou, C.; Yin, H.; Zhou, S. Size-Controlled Synthesis of Highly Stable and Active Pd@SiO₂ Core–Shell Nanocatalysts for Hydrogenation of Nitrobenzene. *J. Phys. Chem. C* **2013**, *117*, 8974–8982. [[CrossRef](#)]
49. Taylor, A. Practical surface analysis, 2nd edn., vol I, Auger and X-ray photoelectron spectroscopy. Edited by D. Briggs & M. P. Seah, John Wiley, New York, 1990, 657 pp., price: £86.50. ISBN 0471 92081 9. *J. Chem. Technol. Biotechnol.* **2007**, *53*, 215. [[CrossRef](#)]
50. Barrett, E.P.; Joyner, L.G. Determination of Nitrogen Adsorption-Desorption Isotherms. *Anal. Chem.* **1951**, *23*, 791–792. [[CrossRef](#)]